

## SUMMARY

- ▶ We analyzed the two outstanding heatwaves (HWs) affecting western and central Europe in late June and late July 2019, respectively.
- ▶ The first HW produced record-breaking temperatures in northeastern Spain and southern France. In this region, temperatures exceeded 45°C.
- ▶ The second HW broke all-time records in large areas of northern France, the Benelux and parts of Germany. For the first time temperatures exceeding 40°C were registered in Belgium and in the Netherlands.
- ▶ We analyzed the large-scale synoptics and driving mechanisms for these summer 2019 events:
  - 1) In both events a subtropical ridge was presented, fostered by a low pressure off in the Atlantic
  - 2) However, while the June HW was controlled by the northward advection of a very warm mass, the July HW presented a larger contribution of regional land-atmosphere diabatic processes.
- ▶ We show how the combined effect of the June HW and a prolonged dry spell in the region contributed to soil desiccation, leading to an amplification of temperature anomalies in late July (further 2°C).
- ▶ We also discuss how these feedback mechanisms are getting stronger in the present due to global warming. Very warm summers with record-breaking events are becoming the “new normal”, even in the absence of extreme dynamical forcing situations, as previously necessary under colder climatic conditions.

## METHODS

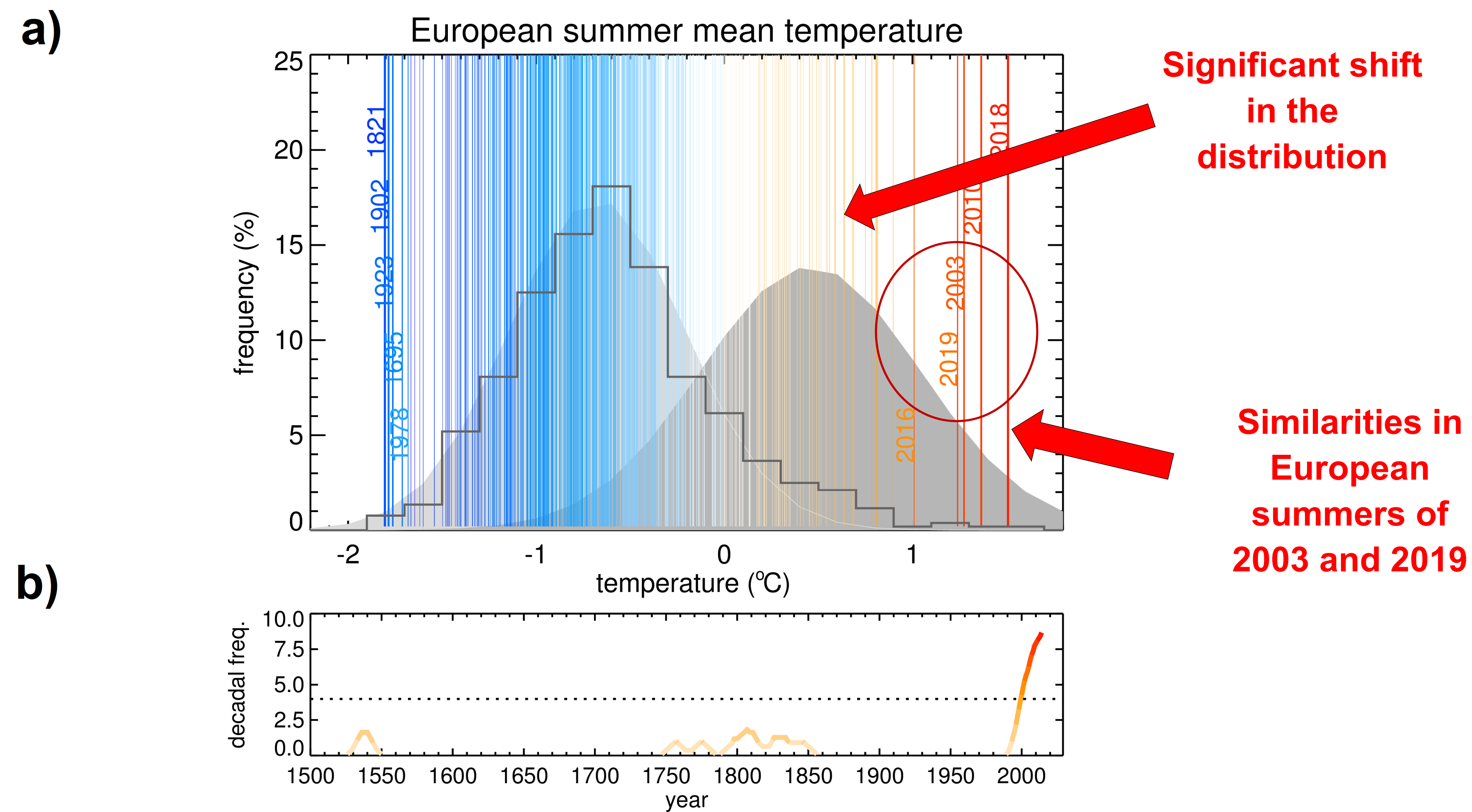
- ▶ A multi-proxy reconstruction for estimates of the European mean summer temperature anomalies since 1500 was used to put the 2019 events into long-term context and also comparing it with the historical 2003 summer.
- ▶ Data from E-OBS was used to characterize and compare the magnitude of anomalies and spatial extent of record-breaking areas in 2019 and 2003, and to see the transient nature of European summer temperatures associated to global warming.
- ▶ The distinct contributions of diabatic and adiabatic forcings (including horizontal and vertical advection) was analyzed for both 2019 HWs, using the NCEP dataset.
- ▶ Satellite derived soil-moisture data (C3S – Copernicus) was combined with meteorological variables from the NCEP dataset to analyze in detail time-series of relevant meteorological indices in specific subdomains.
- ▶ Feedback mechanisms related to latent/sensible heat fluxes were discussed, as well as vertical profiles
- ▶ Two analogues exercises were performed, to check:
  - 1) different near-surface temperature responses to soil moisture pre-conditioning
  - 2) to assess present VS past amplification of soil desiccation in a warming climate

Paper in preparation  
(Sousa et al., 2020)

# The outstanding 2019 Heatwaves in Central Europe : driving mechanisms and soil-atmosphere feedbacks

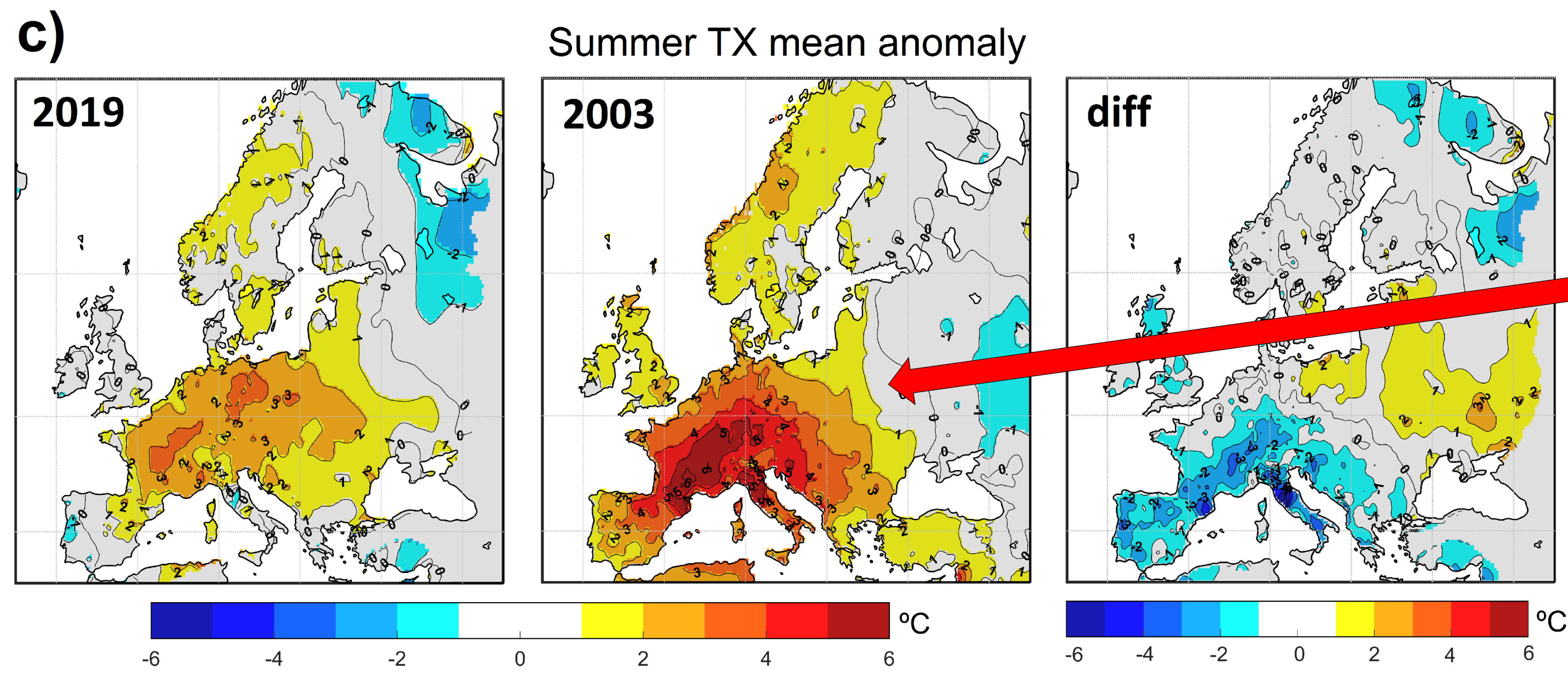
Ricardo M Trigo<sup>(1)</sup>, Pedro M Sousa<sup>(1)</sup>, David Barriopedro<sup>(2)</sup>, Ricardo García-Herrera<sup>(2,3)</sup>, Carlos Ordóñez<sup>(3)</sup>, Pedro MM Soares<sup>(1)</sup>

(1) Instituto Dom Luiz (IDL), Faculdade de Ciências, Universidade de Lisboa, 1749-016 Lisboa, Portugal (rtrigo@fc.ul.pt); (2) Instituto de Geociencias, IGEO (CSIC-UCM), Madrid, Spain; (3) Departamento de Física de la Tierra y Astrofísica, Facultad de Ciencias Físicas, Universidad Complutense de Madrid, Madrid, Spain

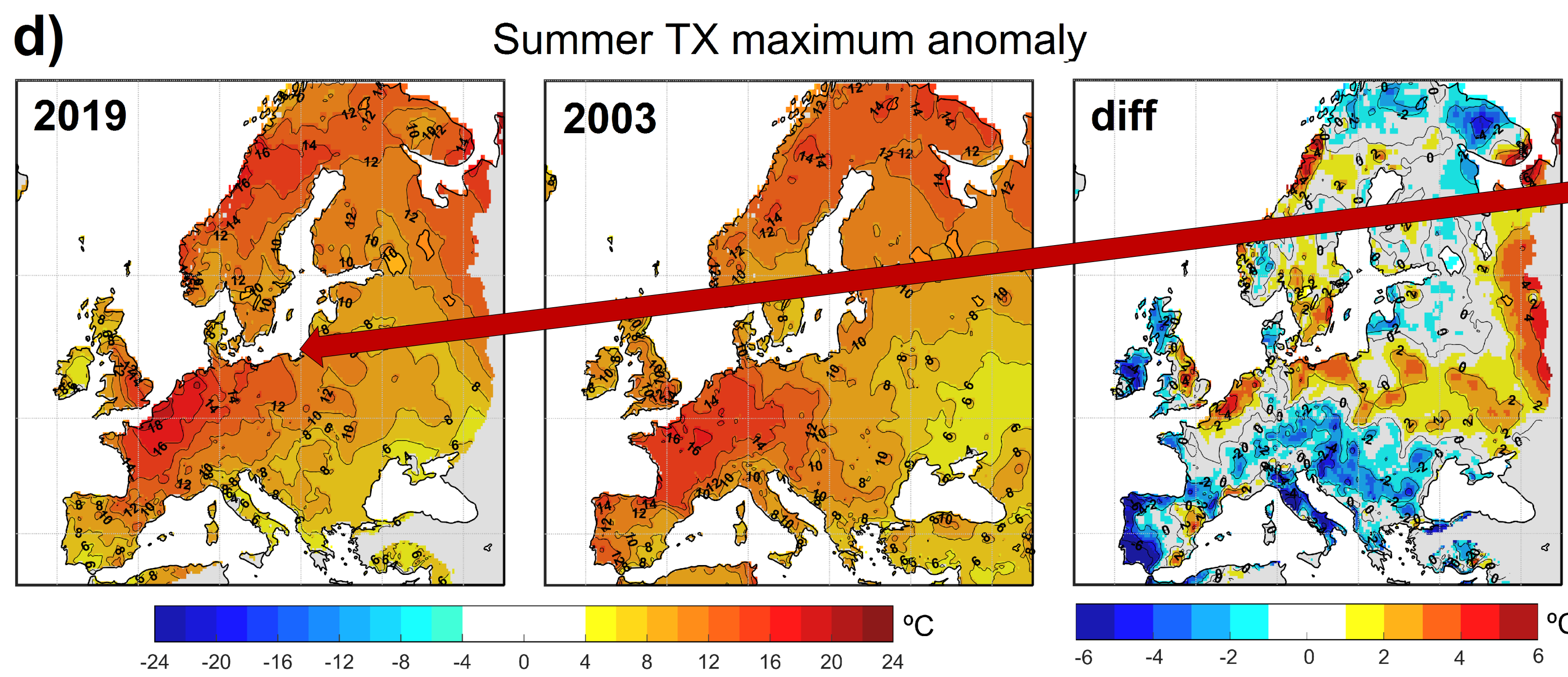


Significant shift in the distribution

Similarities in European summers of 2003 and 2019



Summer 2003 on the overall was more anomalous in relation to the climate normal back then



Summer 2019 absolute anomalies during the heatwave days were more extreme (reaching almost +20°C)

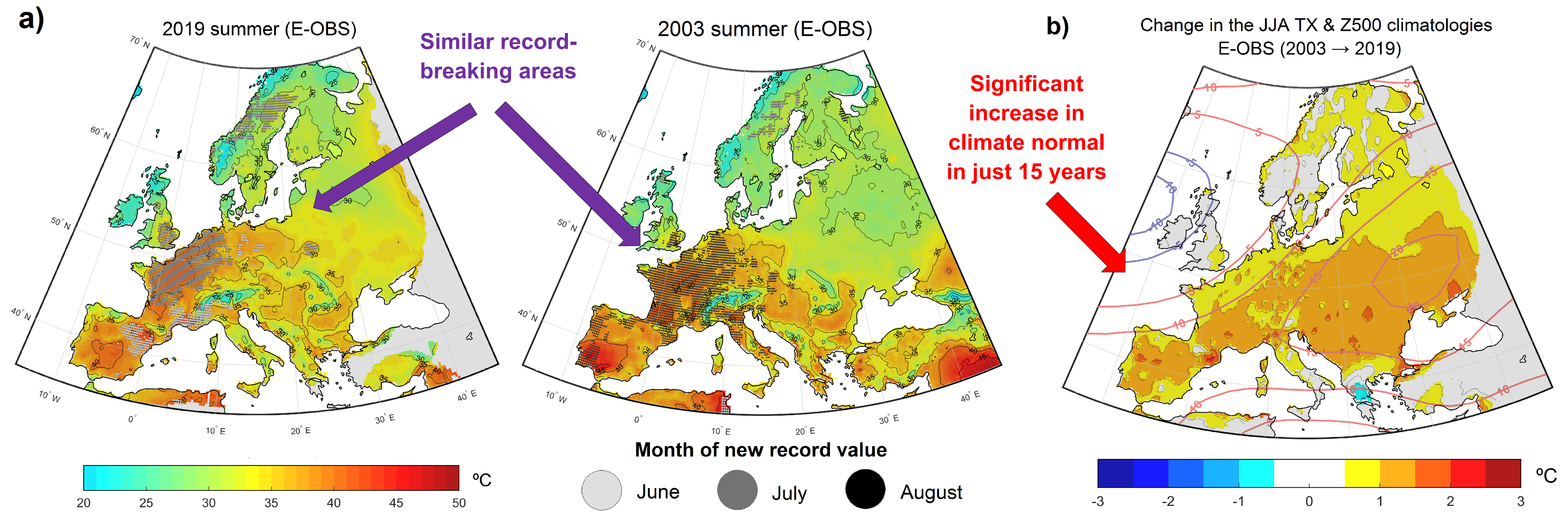


**Fig.2 – The 2019 and 2003 European heatwaves.** a) Maximum daily TX (°C) during summers 2019 and 2003 according to the E-OBS dataset (shading), and areas where all-time records (since 1950) were broken (hatched areas, with grey darkness indicating the month of occurrence). 30-year climatological means), and their difference. b) Difference between 2003 and 2019 moving climatologies of summer TX (shading, °C) and Z500 (solid lines, dam), as defined from their previous 30-yr periods (1973-2002 and 1989-2018, respectively).

Unprecedented northward extension of Saharan intrusion in the June HW

Subtropical ridge & Saharan intrusion extension

Major role of horizontal advection in June

Major role of diabatic processes in July

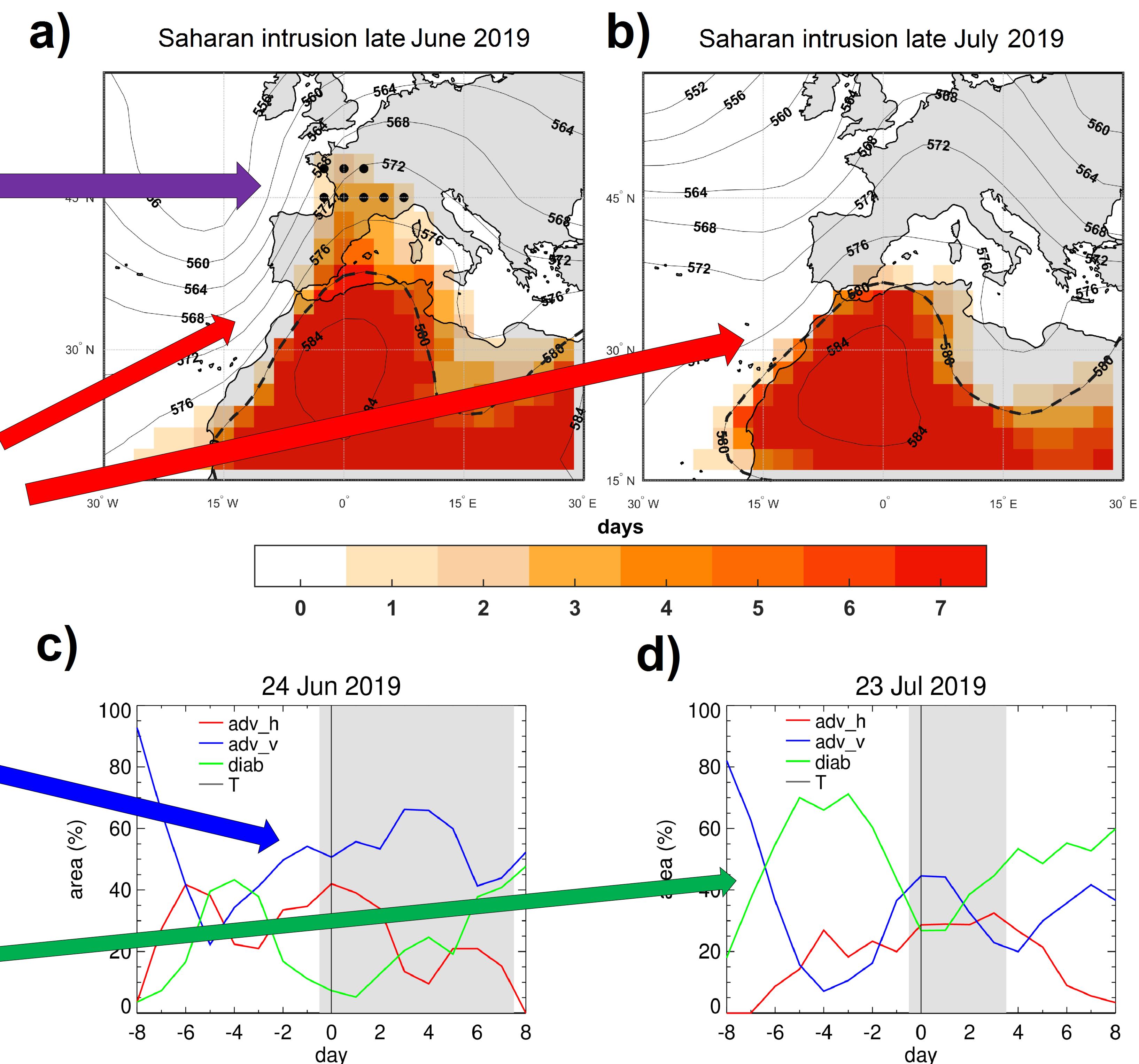


**Fig.3 - Synoptic configuration and forcing mechanisms.** a) Number of days (shading) when a Saharan intrusion was detected in each grid cell during the June HW. Black dots represent areas where such intrusions were unprecedented (since 1948). Lines depict the composite of 1000-500 hPa geopotential height thickness (in m) for the days when our algorithm detects heatwave conditions. b) Same as a), but for the July HW. Grey shading as for previous panels. d) Same as c) but for the July HW.

**Fig.1 - Summer 2019 in Europe.** a) European summer land temperature anomalies (°C, with respect to 1981-2010) for 1500-2019 (vertical lines) and their probability density function (percentage, histogram). The five warmest (coldest) summers of 1500-2019 are highlighted in red (blue). Light (dark) grey shading shows a Gaussian fit of the distribution for 1960-1989 (1990-2019). b) Smoothed running decadal frequency of extreme summers (>95th percentile of 1500-2019), with dotted line showing the maximum decadal value that could be expected by random chance (one side  $p < 0.05$ ). c) Average TX anomalies for the 2019 and 2003 summers (calculated with respect to their corresponding previous 30-year climatological means), and their difference. d) Same as c) but for the highest TX anomalies registered in each summer.

# The outstanding 2019 Heatwaves in Central Europe : driving mechanisms and soil-atmosphere feedbacks

**Ricardo M Trigo<sup>(1)</sup>, Pedro M Sousa<sup>(1)</sup>, David Barriopedro<sup>(2)</sup>, Ricardo García-Herrera<sup>(2,3)</sup>, Carlos Ordóñez<sup>(3)</sup>, Pedro MM Soares<sup>(1)</sup>**  
 (1) Instituto Dom Luiz (IDL), Faculdade de Ciências, Universidade de Lisboa, 1749-016 Lisboa, Portugal (rtrigo@fc.ul.pt); (2) Instituto de Geociencias, IGEO (CSIC-UCM), Madrid, Spain;  
 (3) Departamento de Física de la Tierra y Astrofísica, Facultad de Ciencias Físicas, Universidad Complutense de Madrid, Madrid, Spain

This work was supported by national funds through FCT (Fundação para a Ciência e a Tecnologia, Portugal) under project IMPECAF (PTDC/CTA-CLI/28902/2017).

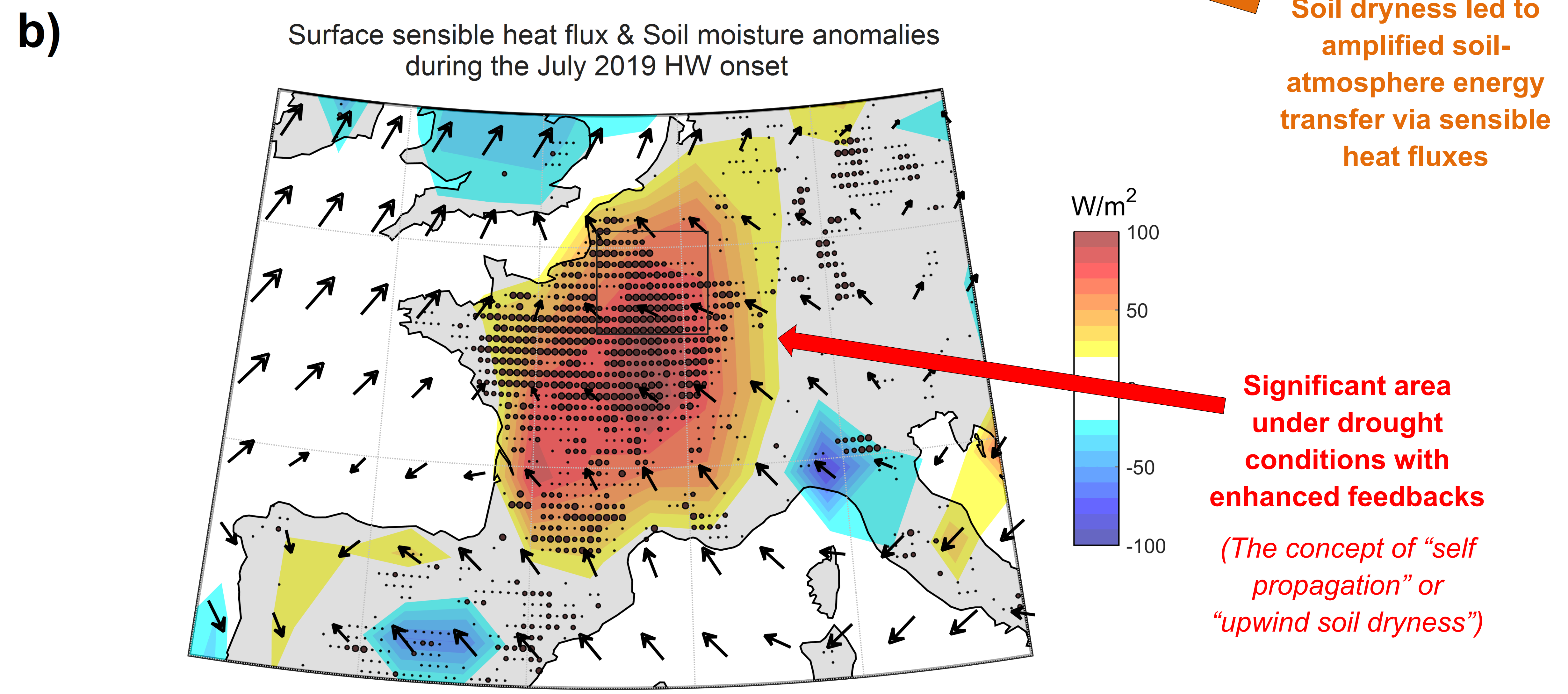
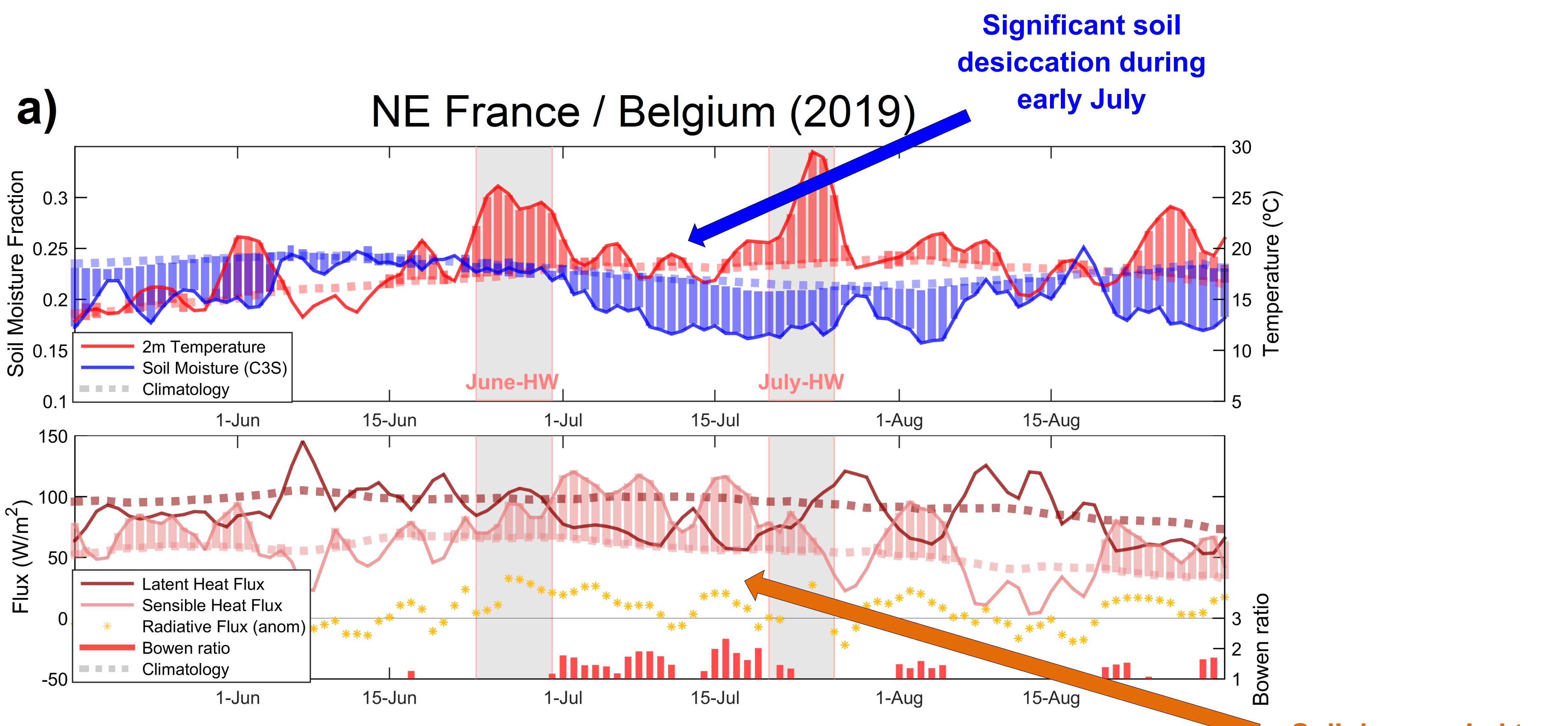


**Fig.4 - Contributions to the July HW.** a) Evolution of a set of variables related to HWs and surface processes, averaged for a regional box over the record-breaking area of the July HW (NE France/Belgium [48°–50.5° N, 2°–6° E]): Upper panel shows 2m temperature (°C) and soil moisture (in fraction), while lower panel shows latent/sensible heat fluxes and net radiative flux anomaly (W/m<sup>2</sup>). Dashed lines represent the climatological value and hatched areas correspond to positive (negative) anomalies for 2m temperature and sensible heat flux (soil moisture). Days with Bowen Ratio above 1 are also presented (red bars in lower panel), illustrating periods where upward fluxes of sensible heat exceed those of latent heat. b) Sensible heat flux anomalies (shading, W/m<sup>2</sup>) averaged during the 7 days prior to the July HW, with vectors depicting the mean near-surface wind during the same period. Dots represent areas with soil moisture deficits (different sizes depict 10%, 20% and 30% deficit), averaged during the 15 days before the July HW onset (here using the C3S satellite derived product). Black box represents the area considered for the series presented in a)..

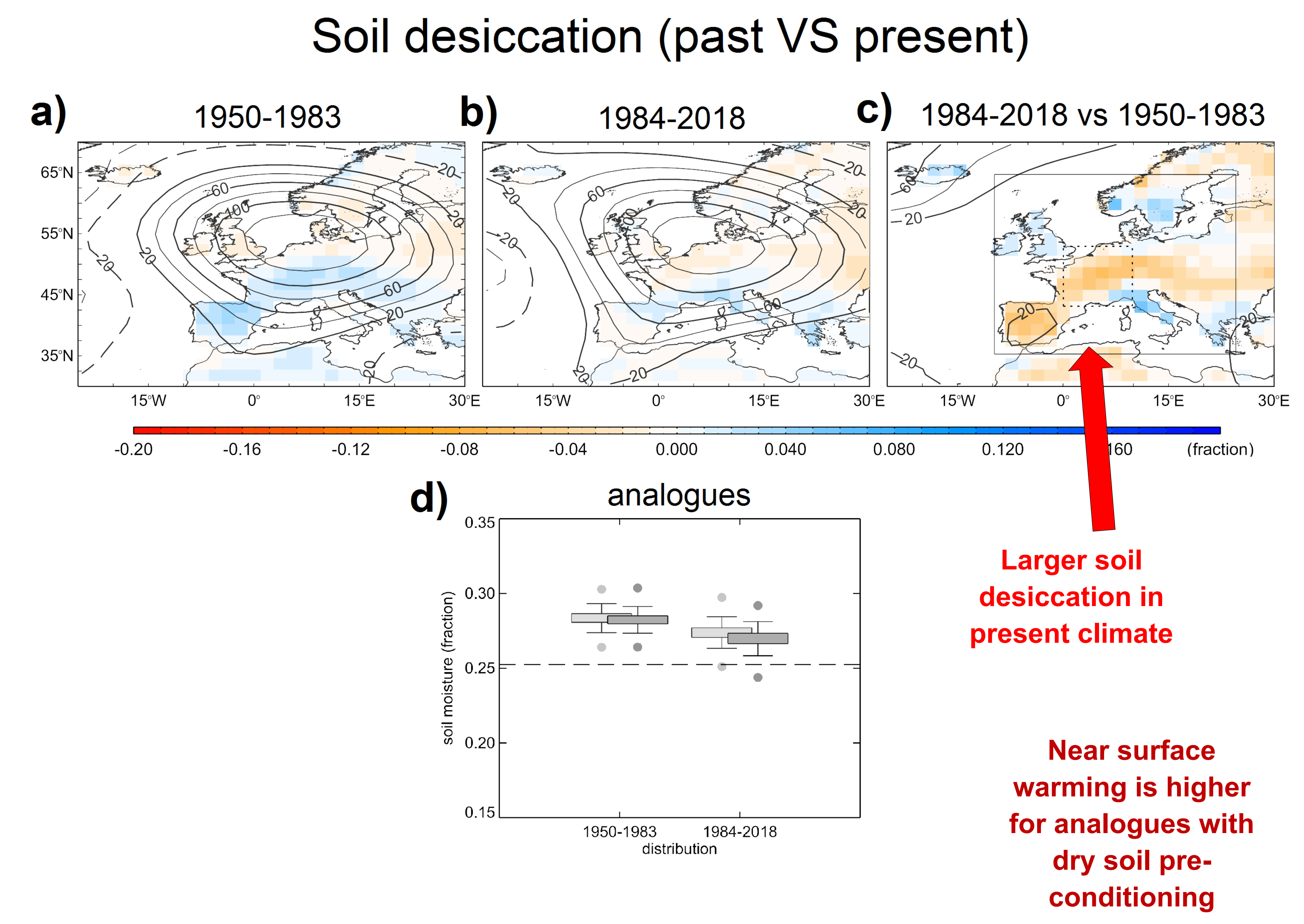


**Fig.5 - Intensified soil desiccation after the June HW.** Mean anomalies (with respect to 1981-2010) of Z500 (m, contours) for the June HW (24 June - 1 July 2019) and soil moisture at 0-10 cm (volumetric fraction, shading) for the 15-day period after the HW (9 July 2 - 16 July 2019), as reconstructed from daily flow analogues of Z500 over Europe (solid box in c) for a) 1950-1983 and b) 1984-2018. c) Difference between b) and a). d) Flow-conditioned (dark grey boxes) and random (light grey boxes) distributions of the mean soil moisture content at 0-10 cm over CEU (dashed box in c) for the same 15-day period during 1950-1983 and 1984-2018 (x-axis). Boxes and whiskers show the  $\pm 0.5$ -SD around the mean and 5th–95th percentile ranges, respectively, with circles denoting the maximum and minimum values. Data source: NCEP/NCAR reanalysis.

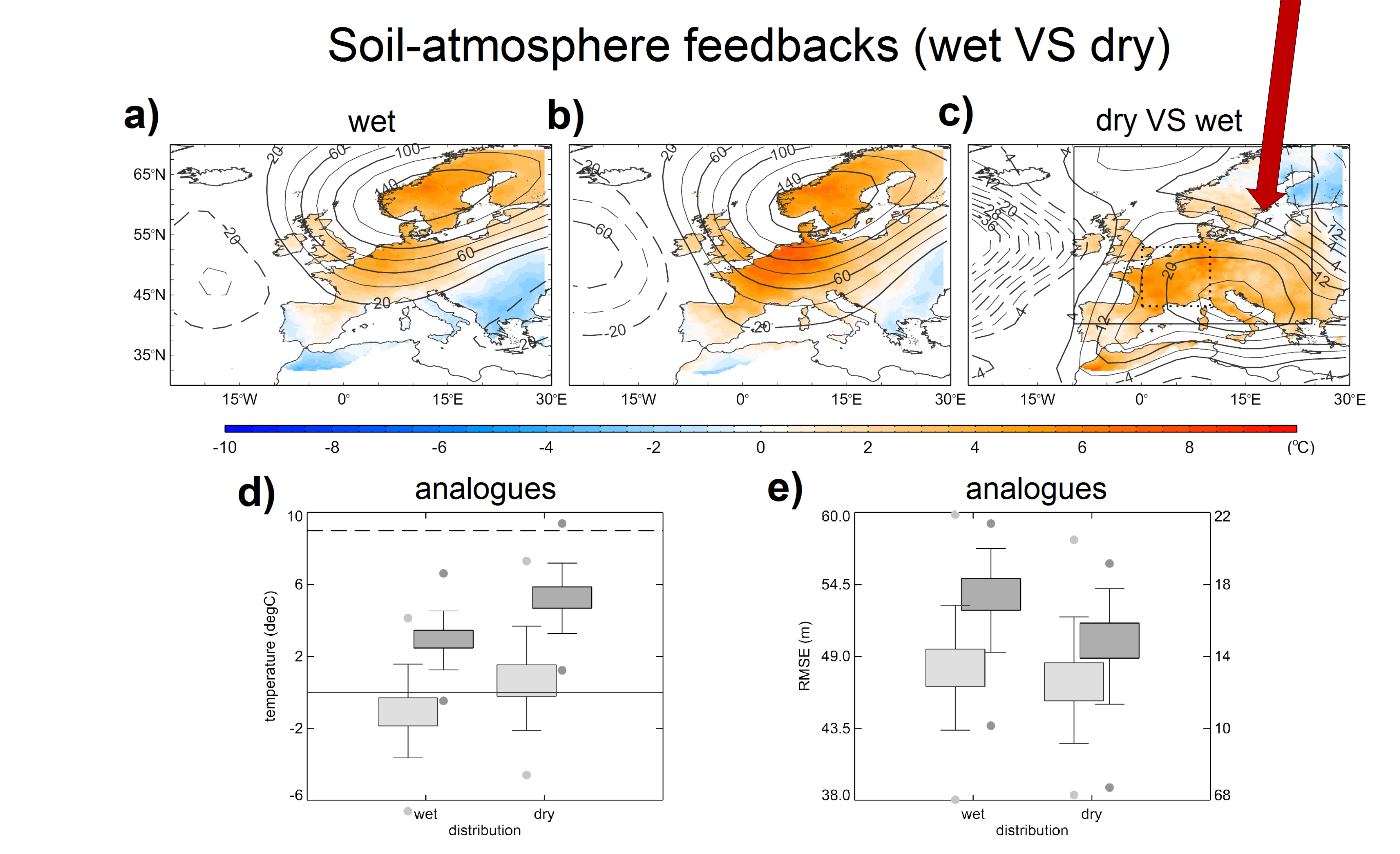


**Fig.6 - Soil-atmosphere feedbacks during the July HW.** Mean Z500 (m, contours) and TX (°C, shading) anomalies (with respect to 1981-2010) reconstructed for the July HW (23-26 July 2019) from daily flow analogues of Z500 over Europe (solid box in c) preceded by a) wet (above 66th) and b) dry (below 33rd) soil moisture conditions at 0-10 cm in CEU (dashed box in c) during the previous 15 days. c) Difference between b) and a). d) Flow-conditioned (dark grey boxes) and random (light grey boxes) distributions of the mean TX anomalies for the July HW over CEU preceded by wet and dry conditions (x-axis). e) As d) but for the root-mean-square error (RMSE) distributions of the flow-conditioned (dark grey boxes, right y-axis) and random (light grey boxes, left y-axis) analogues. Boxes and whiskers show the  $\pm 0.5$ -SD around the mean and 5th–95th percentile ranges, respectively, with circles denoting the maximum and minimum values. Data source: NCEP/NCAR reanalysis..